Nuclear Instruments and Methods 214 (1983) 253–260
North-Holland Publishing Company

CHARGE COLLECTION IN SILICON STRIP DETECTORS

E. BELAU, R. KLANNER, G. LUTZ, E. NEUGEBAUER, H.J. SEEBRUNNER and A. WYLIE
Max-Planck Institut für Physik und Astrophysik, Werner-Heisenberg-Institut, Munich, Fed. Rep. Germany

F. BÖHRINGER, L. HUBBELING and P. WEILHAMMER
CERN, Geneva, Switzerland

J. KEMMER
Technische Universität, Munich, Fed. Rep. Germany

U. KÖTZ *
DESY, Hamburg, Fed. Rep. Germany

M. RIEBESELL **
University of Hamburg, Fed. Rep. Germany

The charge collection in silicon detectors has been studied, by measuring the response to high-energy particles of a 20 μm pitch strip detector as a function of applied voltage and magnetic field. The results are well described by a simple model. The model is used to predict the spatial resolution of silicon strip detectors and to propose a detector with optimized spatial resolution.

1. Introduction

Recently the planar process, developed for producing microelectronics, has been adapted to the fabrication of detectors for ionizing radiation [1]. One of the first applications of this new technology was the development of microstrip detectors with high spatial resolution as a vertex telescope for elementary-particle interactions at high energies [2]. In this work we describe a silicon strip detector with 20 μm pitch and analogue read-out of every channel. The response of the counter to high-energy particles has been measured as a function of applied voltage and external magnetic field. A simple model of charge transport in the detector provides a good description of the measurements. The model is used to calculate the spatial resolution of microstrip detectors and compare it with measurements. A design of a microstrip detector with improved spatial resolution is proposed.

2. The experimental apparatus

2.1. The microstrip detector

A high-ohmic (~ 3 kΩ cm) n-doped silicon crystal, oriented in the 1,1,1-direction, 2 inches in diameter and 280 μm thick, is used as base material. One face of the crystal is aluminized. On the other face the sensitive area of the counter (2 mm × 32 mm) is covered with p^+ implanted diode strips and Al contacts (100 strips of 10 μm width, 32 mm length, and 20 μm pitch). The strips are fanned out to 180 μm pitch directly on the silicon chip (see fig. 1). The counter is glued onto a printed fibre board which fans the signal lines to a pitch of 1/10 inch. Ultrasonic wedge-bonding is used to connect the counter to the fan-out board using 25 μ Al-wire. Further details of the technology are described in refs. 1 and 2.

The functioning of the counter is explained with the help of fig. 2. Connecting the strips to negative voltage depletes the n-doped silicon counter of free charge carriers. Above the depletion voltage of about 120 V an electric field distribution, as shown in fig. 2b, is obtained. A high-energy particle traversing the counter produces approximately 24000 electron–hole pairs in a narrow tube around its path. Under the influence of the

* ...or at CERN, Geneva, Switzerland.
** ...mer student at CERN, Geneva, Switzerland.

...87/83/0000–0000/$03.00

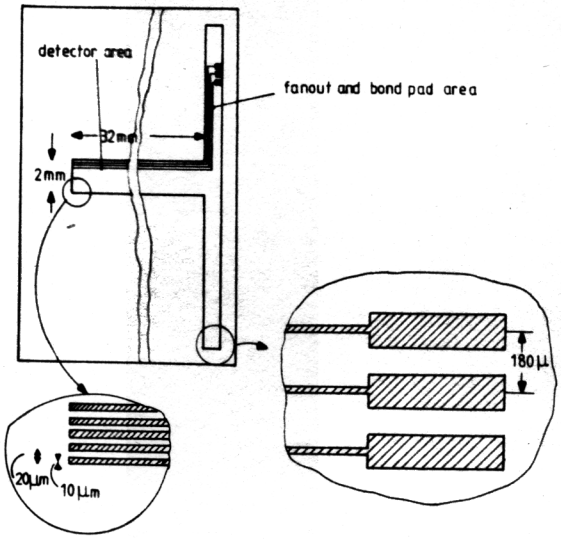

Fig. 1. Layout of the strips on the detector.

electric field, electrons drift towards the ground plane and holes towards the diode strips. During the drift time the narrow tube of charge carriers widens owing to diffusion and electrostatic repulsion. Finally, the holes are collected by the strips. As long as the integration time of the electronics connected to the strips is long compared to the charge collection time, and the dynamic input resistance of the amplifiers is small compared to the interstrip resistance, effects of charge induction cancel and the charge arriving at the read-out strips is measured.

2.2. The electronics chain

The electronics of ref. 2 has been used. Every read-out channel consists of a charge-sensitive FET amplifier and a shaping amplifier which drives a 40 m long twisted-pair cable. The signals are further amplified and coupled via transformers to LRS 2281 voltage-sensitive analogue-to-digital converters (ADCs). The total gain of the electronic chain amounts to 1 V output for an input charge of 4×10^{-15} C (the mean charge deposited by a minimum ionizing particle traversing the counter). The typical r.m.s. noise at the input is 1.2×10^{-16} C.

The relative calibration of the individual channels to within $\pm 2\%$ is performed by injecting test signals into the input of the preamplifier. The calibration was checked using signals from minimum ionizing particles.

2.3. The experimental set-up

The measurements were performed in the H6 beam of the CERN SPS. The trigger counters, as well as the data-acquisition system of the NA11 experiment [3], have been used. Fig. 3 shows a schematic layout of the set-up. The scintillation counters B1 and B2 define the beam and provide signals for the ADC gates. The anticoincidence counter B4 suppresses interacting particles. The silicon counter D is positioned close to the exit of a 1.5 m long bending magnet. The direction of the strip pattern was put parallel to the direction of the magnetic field and normal to the incident beam (fig. 2a). For the measurements only twelve strips of the counters were connected to read-out electronics, yielding an effective counter size of 0.24 mm × 32 mm. The beam spot was 2 mm × 15 mm.

Beam rates were 10^4 counts per second per strip, the beam divergence was ± 1 mrad, and the beam momentum was 200 GeV/c.

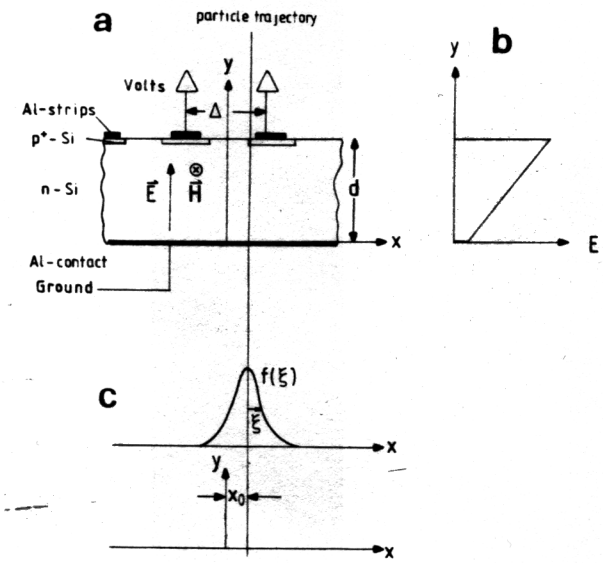

Fig. 2. Layout of the strip detector in the magnetic field; definition of the coordinate system and the parameters used for the measurement of the collected charge distribution. a) Cross-section of strip detector; b) Electric field in detector; c) The distribution of charges.

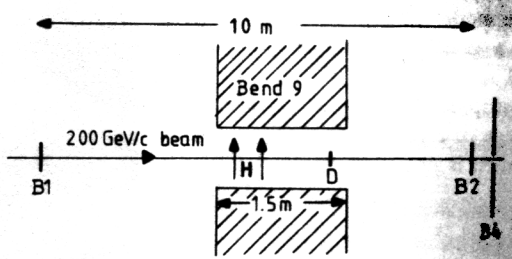

Fig. 3. Schematic of layout of the experimental set-up.

3. Results

In subsection 3.1 we shall present measurements of quantities such as the distributions of pulse height and cluster width, and give a qualitative discussion of their dependences on applied voltage and magnetic field. In subsection 3.2 we shall use the measurements to determine the spatial distribution of the charge arriving at the strips.

3.1. Pulse height and cluster-size distribution

Data have been taken at voltages of 120 V (the measured depletion voltage), at 200 V, and at values of 0, 1.32, and 1.68 T for the magnetic field.

Events corresponding to particles traversing the detector were selected off line by demanding a pulse height of at least 25% (channel No. 200 of the ADC) of the mean pulse height of a minimum ionizing particle (MI) in at least one of the strips. For these events a cluster is defined as a group of adjacent channels each with at least 10% MI. The number of channels above this threshold is called cluster size. The cluster pulse height is the sum of pulse heights in the cluster. To avoid edge effects, events are discarded if the maximum pulse height in a cluster is in one of the outer channels of the counter.

The results of the measurements for a counter voltage of 120 V (depletion voltage) and 200 V, and for magnetic field values of 0, 1.32, and 1.68 T are presented in table 1 and fig. 4. We note the following:

i) Above the depletion voltage of 120 V the mean pulse height and the width of the pulse-height distribution are independent of applied voltage and magnetic field.

ii) The cluster-size distribution varies significantly as a function of applied voltage and magnetic field. Increasing the voltage decreases the average cluster size, as expected from the decreased collection time, which reduces the effect of diffusion of the collected charge carriers. A magnetic field perpendicular to the direction of the drifting charges and parallel to the read-out strips increases the average cluster size, as expected from the effect of the Lorentz force.

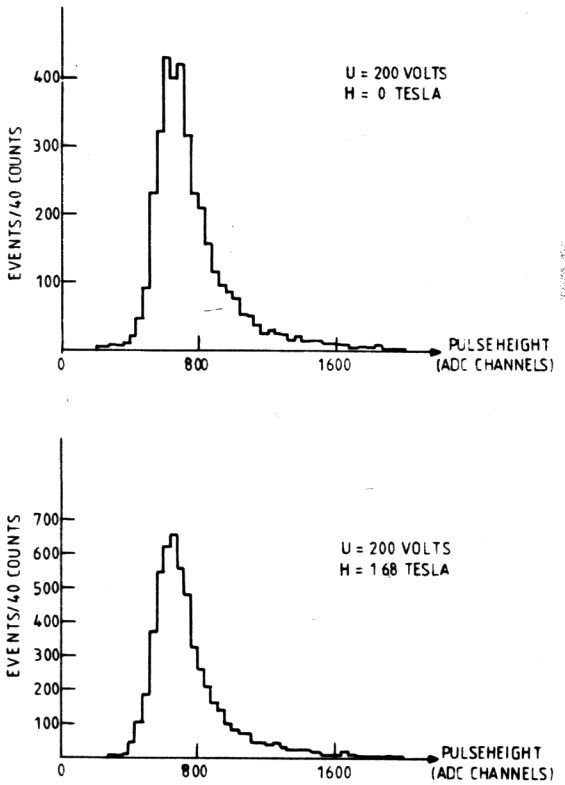

Fig. 4. Pulse-height distribution for high-energy particles with and without external magnetic field.

3.2. The shape of the collected charge distribution

In this subsection we present a method which allows the determination of the spatial distribution of the holes

Table 1
Pulse-height and cluster-size distribution as a function of electric and magnetic field in a 20 μm silicon counter [a]

Applied voltage (V)	Applied H fields (T)	Mean pulse height (ADC channels)	Full width of pulse-height distribution (ADC channels)	No. of events	Percentage of events with cluster size [b]		
					1	2	≥ 3
120	0	760 ± 4	250	3752	40.6%	53.9%	5.3%
200	0	766 ± 4	240	3677	47.2%	48.4%	4.3%
120	1.32	762 ± 5	240	2638	21.2%	73.9%	5.2%
120	1.68	755 ± 4	250	6929	15.7%	79.8%	4.5%
200	1.68	764 ± 4	240	5269	24.8%	70.2%	5.0%

[a] Errors indicated are statistical only.
[b] For definition of cluster size, see subsection 3.1.

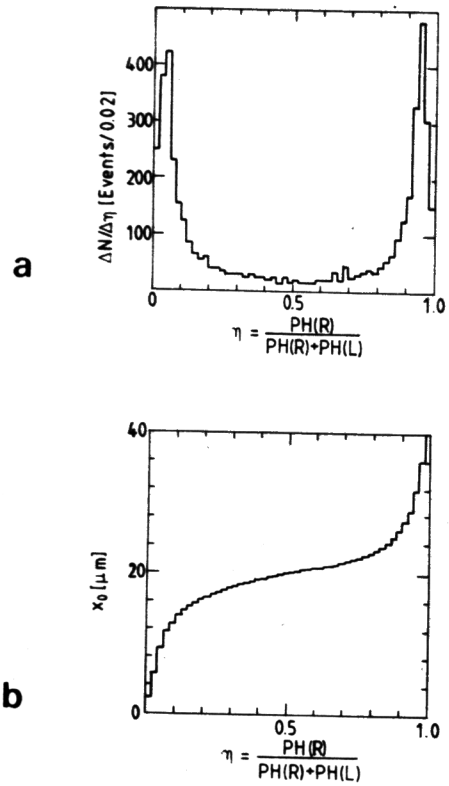

Fig. 5. Experimental distributions for $U = 200$ V, $H = 0$ T. a) $\Delta N/\Delta\eta$; see text for definition of η; b) the relation between x_0, the impact point of the particle and η, the measured pulse-height ratio obtained from the integrated histogram of (a).

collected at the read-out strips. The counter is irradiated uniformly with high-energy particles and for every event the values of the pulse height (PH) of the individual strips are recorded. Energetic δ electrons are removed by rejecting events with a pulse height exceeding 1.7 minimum ionizing particles. A sample of events with particles traversing the counter between strips L and R are selected by demanding that the centre of gravity of the pulse heights is between strips L and R *. For these events the quantity

$$\eta = \frac{\mathrm{PH(R)}}{\mathrm{PH(L)} + \mathrm{PH(R)}} \qquad (1)$$

is calculated. Fig. 5a shows as an example $\mathrm{d}N/\mathrm{d}\eta$, the

* After rejecting δ electrons by the pulse-height cut, we observe that the entire charge deposited by a particle is contained in at most four strips. In the analysis the pulse heights of neighbouring 20 μm wide strips are added in order to obtain effectively a counter of $\Delta = 40$ μm wide strips. L and R refer to these 40 μm strips. Thus PH(L)+PH(R) contains the entire pulse height deposited by a particle. This is assumed in the further derivation of the method.

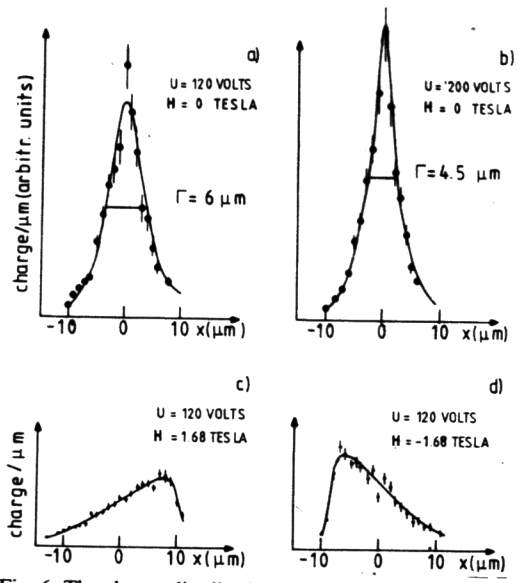

Fig. 6. The charge distribution collected by the diode strips: a) $U = 120$ V, $H = 0$ T; b) $U = 200$ V, H = 0 T; c) $U = 120$ V, $H = 1.68$ T; d) $U = 120$ V, $H = -1.68$ T.

distribution of η for the data taken at 200 V with zero magnetic field. The average impact point x_0 for a given η can be obtained by (fig. 2):

$$x_0 = \frac{\Delta}{N_0}\int_0^{\eta}\frac{\mathrm{d}N}{\mathrm{d}\eta}\mathrm{d}\eta - X_0. \qquad (2)$$

For the derivation we have assumed that N_0 particles, uniformly distributed in x_0, have traversed the counter in the interval of width Δ between strips L and R. X_0 is a constant which relates the origin of the η scale to the origin of the x_0 scale. Without magnetic field we expect the deposited charge to spread symmetrically around the particle trajectory – in this case $X_0 = \Delta/2$. In the analysis we use the cumulative $\mathrm{d}N/\mathrm{d}\eta$ distribution to obtain x_0 for every η value, as shown in fig. 5b.

The distribution $\mathrm{d}N/\mathrm{d}\eta$ can also be used to determine $f(\xi)$ **, the distribution of charge carriers around the impact point of the particle arriving at the read-out plane. For a particle traversing the counter at x_0, the measured pulse heights are related to $f(\xi)$ by

$$\mathrm{PH(L)} \propto \int_{-\infty}^{-x_0} f(\xi)\mathrm{d}\xi, \qquad \mathrm{PH(R)} \propto \int_{-x_0}^{\infty} f(\xi)\mathrm{d}\xi.$$

Using the definition of η we obtain

$$\frac{\mathrm{d}\eta}{\mathrm{d}x_0} = f(-x_0).$$

Having again N_0 particles, uniformly distributed in x_0 in

** $f(\xi)$ is the one-dimensional projection of the charge distribution, normalized so that $\int_{-\infty}^{+\infty} f(\xi)\mathrm{d}\xi = 1$.

the interval Δ, we obtain

$$\frac{dN}{d\eta} = \frac{dN}{dx_0}\frac{dx_0}{d\eta} = \frac{N_0}{\Delta}\frac{1}{f(-x_0)}. \quad (3)$$

Eq. (2) allows us to determine for every η bin the value of x_0. Using eq. (3) the corresponding value of $f(x_0)$ can be obtained.

The above method is limited by statistical fluctuations. They are mainly due to electronics' noise and δ electrons. Therefore events with δ electrons have to be removed from the analysis with a cut on the cluster pulse height. The tails of the charge distribution cannot be determined with this method, owing to electronics noise, which amounts to about 3% of the pulse height of minimum ionizing particles.

Fig. 6 shows the charge distributions $f(\xi)$ determined using the above method for various voltages and magnetic fields. The solid lines are fits described in the next subsection.

Without magnetic field the charge distribution is symmetric with a full width of 6 μm at 120 V, decreasing to 4.5 μm at 200 V. The width is sufficient to lead to charge interpolation for a counter with 20 μm pitch. This explains why the r.m.s. spatial resolution of 4.5 μm, found experimentally in ref. 2 for 20 μm pitch counters, is smaller than the value naively expected from the pitch of 20 μm (20 μm/$\sqrt{12}$ = 5.8 μm).

An asymmetric charge distribution is obtained if the magnetic field is switched on. A field of 1.68 T introduces a systematic shift of the measured coordinate of the order of 10 μm (for a 280 μm thick counter) and an increase in the width of the collected charge distribution from 5 to approximately 12 μm. For a more detailed discussion we refer to the next subsection.

3.3. Determination of Lorentz angle and diffusion

We use a simple model to describe the spatial distribution of the collected charge, which will allow us to determine

δ: the r.m.s. width of the initial charge distribution;

D_h: the transverse diffusion constant of holes in silicon;

μ_H: the Hall mobility * of holes related to the drift angle θ_L with respect to the direction of the electric field, due to their drift in the external magnetic field H by $\tan\theta_L = \mu_H H$.

We assume that the initially produced charge distribution drifts under the influence of electric and magnetic fields to the read-out strips – diffusion results in a widening of the charge distribution; the magnetic field causes the charges to drift at an angle θ_L with respect to the direction of the electric field.

The electric field inside the fully depleted counter is obtained by solving the Poisson equation (see fig. 2 for definition of symbols) yielding:

$$E(y) = \left[\frac{U - U_D}{d} + \frac{2U_D y}{d^2}\right],$$

$$\boldsymbol{E} = (0, E, 0),$$

where U_D is the magnitude of depletion voltage; U is the magnitude of applied voltage ($U \geq U_D$ for depletion); d is the counter thickness. The time it takes for a charge generated at the point $y = y_0$ to drift to the read-out strips located at $y = d$ is obtained by integrating the relation between drift velocity v and electric field

$$v = dy/dt = \mu E(y),$$

where μ is the drift mobility of the collected charge carriers. The result is

$$t(y_0) = -\frac{d^2}{2\mu U_D}\ln\left(1 - \frac{2U_D(d - y_0)}{(U + U_D)d}\right). \quad (4)$$

We assume that a minimum ionizing particle traverses the counter at time $t = 0$ along the path $x = z = 0$ and deposits one unit of charge distributed uniformly along y and as a δ-function in x and z. In the absence of an electric field and recombination, diffusion leads to a charge density distribution for times $t \geq 0$ *:

$$C(x, y, z, t) = \frac{1}{4\pi D_h t d}\exp\left[-\frac{x^2 + z^2}{4D_h t}\right],$$

for $0 \leq y \leq d$.

Integrating over z, the coordinate along the read-out strips, we obtain

$$C(x, y, t) = \int_{-\infty}^{\infty} C(x, y, z, t)\,dz$$

$$= \frac{1}{\sqrt{4\pi D_h t}\,d}\exp\left(-\frac{x^2}{4D_h t}\right). \quad (5)$$

The effect of a finite width of the primary produced charged distribution can be taken into account, by replacing in eq. (5) the time t by $t + t_0$, with $\delta = \sqrt{2D_h t_0}$ being the r.m.s. radius of the primary produced charge distribution. We thus have

$$C(x, y, t) = \frac{1}{\sqrt{4\pi D_h(t + t_0)}\,d}\exp\left[\frac{-x^2}{4D_h(t + t_0)}\right],$$

for $0 \leq y \leq d$. (6)

* For a definition of Hall mobility see, for instance, Shockley [4]. This book also discusses that, in first approximation, the Lorentz angle θ_L is independent of electric field, which is assumed in our simple model.

* It has been checked that the effect of electrostatic self-repulsion of the charge cloud can be neglected relative to the effect of diffusion for the charge density produced by a minimum ionizing particle.

Under the effect of an electric field in the y direction and a magnetic field in the z direction parallel to the read-out strips, the charges drift at an angle $\tan\theta_L$, relative to the y direction. This we include by replacing x by $x - y\tan\theta_L$. Integrating eq. (6) along y we obtain for the distribution of charges at the read-out strips,

$$f(x) = \frac{1}{\sqrt{4\pi D_h}\, d}\int_0^d \frac{dy}{\sqrt{t+t_o}} \times \exp\left(-\frac{(x - y\tan\theta_L)^2}{4D_h(t+t_0)}\right).$$

t is related to y according to eq. (4).

This function has been fitted by the least squares method to the charge distributions presented in subsection 3.2. The following constants have been used: $U_D = 120$ V; $d = 280$ μm; $\mu = 450$ cm^2/Vs (drift mobility of holes from ref. 5) The free parameters are T_h: the effective hole temperature related to the diffusion constant by the Einstein equation $D_h = kT_h\mu/q$ (ref. 5) (where k is the Boltzmann constant and q the elementary charge); t_0: as described in the text; θ_L: drift angle with respect to the direction of the electric field; X_0: the constant of formula (2) which determines the origin of the x scale.

The function $f(x)$ provides a good description of the measurements, as can be seen from fig. 6, where the results of the fit are drawn as solid lines.

From the data without magnetic field and 120 V we obtain: $T_h = 390 \pm 40$ K; $t_0 = 0.65 \pm 0.35$ ns; $\tan\theta_L = (4.7 \pm 2.0)\times 10^{-3}$.

The errors indicated are the statistical errors; no attempt was made to estimate systematic errors. The finite but small value of $\tan\theta_L$ is fully compatible with a possible non-perpendicular incidence of the beam onto the counter. The values of t_0 are within two standard deviations compatible with zero. They result in a radius of the primary produced charge tube of 1.4 ± 0.7 μm. The value of t_0 and T_h are strongly correlated – fixing t_0 at zero yields for T_h a value of 440 ± 30 K and an increase of χ^2 of 3.5 units. The value found for T_h also depends on the pulse-height cut used to remove electrons. The statistics of the data are not sufficient to investigate this effect further. The effect of δ electrons is to increase the width of the charge distribution resulting in an increase of T_h. We think that the value found by us for T_h represents an upper limit, the true value being closer to the ambient temperature of 300 K. This is also expected from diffusion measurements in high ohmic silicon [6].

The values of θ_L and the Hall mobility are shown in table 2, as a function of magnetic field. Small corrections for the non-normal incidence of the particles onto the counter due to geometrical misalignment and the bending of the particles in the magnetic filed have been applied. Errors indicated are statistical. Within errors the measured Lorentz angle is independent of the electric field and proportional to the magnetic field. Averaging our measurements we obtain a value of (310 ± 15) cm^2/Vs for the Hall mobility of holes in silicon, and a ratio of Hall to drift mobility of 0.69 ± 0.03. This value is in agreement with Hall effect measurements [7], which yield a value around 0.72.

The good description of the data by our simple model and the fact that the fitted parameters are within the expected range give us confidence that the model provides a realistic description of the charge collection in silicon counters.

4. Applications of the results

In this section we use the results from the previous subsection to discuss the properties of silicon counters in magnetic fields and to predict the spatial resolution expected for various silicon strip detector arrangements.

4.1. Influence of magnetic fields on silicon strip detectors

A magnetic field H perpendicular to the direction of the electric field in the counter and parallel to the read-out strips results in a drift angle of $\tan\theta_L = \mu_H H$, with μ_H being the Hall mobility of the collected charge

Table 2
Lorentz angle and Hall mobility for holes in silicon versus magnetic field

Voltage (V)	Magnetic field (T)	$\tan\theta_L \times 10^3$ measured	$\tan\theta_L \times 10^3$ corrected [a]	μ_H (cm^2/Vs)
120	0	$+4.5 \pm 1.5$	-2 ± 3.5	–
200	0	$+0.5 \pm 1.5$	$+2 \pm 3.5$	–
120	1.68	$+58 \pm 2.5$	$+52 \pm 4.5$	310 ± 30
200	1.68	$+56 \pm 2.0$	$+50 \pm 4.0$	300 ± 25
120	1.32	$+51 \pm 2.0$	$+46 \pm 4.0$	350 ± 25
120	−1.68	-50 ± 2.0	-48 ± 4.0	290 ± 25

[a] Corrected for the measured angle for zero magnetic field $[(-2.5 \pm 1)\times 10^{-3}]$ and the deflection of the beam by the magnetic field [e.g. at 1.68 T $(4.0 \pm 1.0)\times 10^{-3}$].

carriers. Typical values for μ_H are [7] 310 cm^2/Vs for holes and 1650 cm^2/Vs for electrons. For a 280 μm thick counter in a 1.5 T field this results in a systematic shift of 6.5 μm (35 μm) of the measured coordinate if holes (electrons) are collected. At the same time the width of the collected charge distribution increases to about twice these values. These effects have to be considered if high-resolution silicon counters are used in magnetic fields.

4.2. The spatial resolution of silicon strip detectors

In this subsection we use the model of section 3 to predict the spatial resolution of silicon strip detectors and compare the results with experimental measurements. The different types of detectors are listed in table 3. They are all made of 3 kΩ cm n-type silicon crystals, 280 μm thick, with 20 μm pitch of the strips but with different read-out pitch and diode arrangements. A voltage of 120 V, just above depletion, is assumed.

The spatial resolution depends on the distance of the particle from the strips. In the following the average resolution is calculated using Monte Carlo techniques. Particles with normal incidence are uniformly distributed between the strips and the sharing of charge between strips is calculated using the model of the previous section. A value of 300 K is used for T_h. For the counters with the read-out pitch larger than the strip pitch (capacitative charge division [2]), losses of charge to ground due to capacitative coupling are taken into account [8]. The charge collected by the read-out strips is smeared by a Gaussian function corresponding to the electronics noise of our set-up (0.12 fC compared to 4 fC of charge deposited). The particle position is estimated from the centre of gravity of the charges on the read-out strips. The distribution of the difference of this estimate and the generated position of the particle yields the resolution.

For counter types b and c we can compare the calculated resolution with measured values. The agreement is satisfactory. The value expected for counter type a of 2.8 μm seems to be close to the best resolution obtainable with strip detectors for minimum ionizing particles – at the 1 μm level we expect fluctuations in the centre of gravity of the deposited charge, due to δ electrons, to dominate the resolution.

A significant improvement in resolution for a given pitch of the read-out electronics is expected for counters of types d, e, and f. For these counters the strips are opposite to the diode, resulting in an electric field decreasing towards the strip. As a result all electrons collected by the strips have to drift through the low-field region, and the increased diffusion yields a charge distribution of a full width of 15 μm. This increased width results in the improved resolution.

5. Conclusions

We have measured the response of a 20 μm pitch silicon strip detector to high-energy particles as a function of applied voltage and magnetic field. The data allow the determination of the spatial distribution of the charge collected by the strips. The results are compared with a simple model which includes the finite width of the produced charge tube, diffusion, and the change of the drift direction due to the Lorentz force. The data are well described by this model and the parameters are found to agree with expectations. The model is used to calculate the spatial resolution of strip detectors – good agreement with existing measurements is found. A different arrangement of diode and strips is proposed which should result in an improved spatial resolution.

It can be concluded that silicon strip detectors can achieve high resolution in magnetic fields in the 1–2 T range if holes are collected by the strips. Problems due to large values of the Lorentz angle can arise if electrons are collected by the strips.

We are indebted to P. Šolc of the Max-Planck Institut in Munich for mounting and bonding the detec-

able 3
patial resolution for various silicon strip detector arrangements with 20 μm strip pitch

Detector type	Read-out pitch (μm)	Diode arrangement	Calculated resolution (μm)	Measured resolution (μm)
	20	strip side	2.8	–
	60	strip side	3.6	4.5
	120	strip side	5.9	7.9
	20	opposite to strips	0.8	–
	60	opposite to strips	2.8	–
	120	opposite to strips	5.6	–

tors and to L. Bonet of CERN for his help in setting up the apparatus. The work would not have been possible without the help we received from the NA11 Collaboration at CERN.

References

[1] J. Kemmer, Nucl. Instr. and Meth. 169 (1980) 449.
[2] B. Hyams et al., Nucl. Instr. and Meth. 205 (1983) 99.
[3] Amsterdam (NIKHEF)–Bristol–CERN–Cracow–Munich (MPI)–Rutherford Collaboration, Measurement of charmed particle production in hadronic reactions, Proposal CERN/SPSC/78-14, SPSC P95 (1978).
[4] W. Shockley, Electrons and Holes in Semiconductors (V Nostrand, Princeton, N.J., 1950).
[5] S.M. Sze, Physics of Semiconductor Devices (Wiley, N York, 1981) 2nd ed.
[6] G. Persky and D.J. Bartelink, J.Appl. Phys. 42 (1971) 44
[7] Landolt-Börnstein, Gruppe III, Band 17a (Springer, Berl 1982), pp. 68, 380 and references quoted.
[8] R. Hofmann, Diplomarbeit Technische Universität, Munic 1982, unpublished.
J. Kemmer et al., in: Proc. of the FNAL Workshop o Silicon Detectors for High Energy Physics (October, 198 ed., T. Ferbel.